Journal of Solid State Chemistry **145,** 452–459 (1999)
Article ID jssc.1999.8147, available online at http://www.idealibrary.com on IDEAL®

3D Long-Range Magnetic Ordering in Layered Metal–Hydroxide Triangular Lattices 25 Å Apart

M. Kurmoo,*,[1] P. Day,† A. Derory,* C. Estournès,* R. Poinsot,* M. J. Stead,‡ and C. J. Kepert‡,[2]

*Institut de Physique et Chimie des Matériaux de Strasbourg, 23 rue du Loess, 67037 Strasbourg Cedex, France; †Royal Institution of Great Britain, 21 Albemarle Street, London W1X 4BS, UK; and ‡Inorganic Chemistry Laboratory, Oxford University, South Parks Road, Oxford OX1 3QR, UK
E-mail: Kurmoo@friss.u-strasbg.fr

Received September 4, 1998; in revised form December 30, 1998; accepted January 5, 1999

The synthesis, characterization, and magnetic properties of the layered compounds, $Cu_2(OH)_3(C_{12}H_{25}SO_3)\cdot H_2O$, $Ni_2(OH)_3(C_{12}H_{25}SO_3)\cdot H_2O$, and $Co_5(OH)_8(C_{12}H_{25}SO_3)_2\cdot 5H_2O$, with a triangular magnetic lattice are reported. The interlayer distances are 23.8 (Cu), 23.0 (Ni), and 25.8 Å (Co). Long-range ferromagnetic (Ni) and ferrimagnetic (Co) ordering are observed with Curie temperatures of 18 (Ni) and 50 K (Co). The coercive fields are 400 (Ni) and 19,000 Oe (Co), the latter being among the hardest metal–organic magnets. The long-range ordering is interpreted as being due to dipolar interaction between layers with large effective moments as a consequence of precursor short-range intralayer interactions. The large coercive field is interpreted as resulting from a synergy of crystalline shape, surface, and single ion anisotropies.

INTRODUCTION

Inorganic layered compounds are of current interest because of their ability to host large guest molecules which have specific functions (1–5). A range of host materials are available with various intrinsic physical characteristics. These include clays, double hydroxides, metal halides, oxides, sulfides, and phosphates (5, 6). Both neutral and charged (anionic and cationic) organic or inorganic guests having specific properties can be inserted. They are used as supports for catalysts and to bring molecules close enough so that photochemical reactions, e.g., [2 + 2] cycloaddition, *cis–trans* isomerization, and polymerization, can be performed in the solid (6–8). Other uses include water purification, ion exchange, chromatography, and as electrodes (9–11). These applications are due principally to their intrinsic structures which consist of sheets formed via strong covalent bonding but having only weak interlayer forces. They have also been used as precursors to bimetallic compounds, as one is able to control the relative proportion of each metal.

Layered double hydroxides (LDH) are of particular interest and have been used extensively as hosts (12–14). The structure of LDH are very similar to that of brucite, $Mg(OH)_2$. Magnesium is in octahedral coordination with six oxygen ions in the form of hydroxide; the octahedral units then, through edge sharing, form infinite sheets. The sheets are stacked on top of each other through hydrogen bonding. When some of the magnesium in the lattice is replaced by a higher positively charged cation, the resulting overall single layer (e.g., Mg–Al–OH) gains a positive charge. Sorption of an equivalent amount of hydrated anions renders the structure electrically neutral. The anions are therefore not bonded to the metal. Many of these are known in nature where the anions are frequently found to be the carbonate ion, although sulfate, OH, and Cl are occasionally found. It is equally possible to have covalently bonded anions by replacing one of the hydroxides with a carboxylate for example.

From a magnetic point of view, these compounds are of interest for three main reasons. Firstly, the triangular arrangement of the spin carriers is of theoretical importance with regard to frustration problems (15). In addition, the question of long-range order in two dimensions has been a subject of great interest, from a theoretical as well as an experimental point of view (16). Secondly, the possibility of introducing guest molecules in the galleries between the layers provide a way to tune one magnetic exchange independently while keeping those within the layer unaltered. Furthermore, it also allows one to introduce other spin carriers (17), optically active molecules and electron or hole carriers for creating structures with combined properties. Thirdly, when the layers are well separated one can consider them as multiple replicas of single layer magnets. If the moments have perpendicular alignment they can be of great commercial value for high-density

[1] To whom correspondence should be addressed.
[2] Present address: School of Chemistry, University of Sydney, NSW 2006, Australia.

0022-4596/99 $30.00

magnetic recording materials, an area of research which is very active (18).

We have prepared a series of magnetic layered compounds based on the rigid brucite-like metal–hydroxide triangular lattice (M–M distance of ca. 3 Å (19)) where the interlayer separation can be tuned from 9 to 29 Å by changing the shape and size of the anion, for example, the alkyl chain length of the anion separating the layers. Several anions containing carboxylate, dicarboxylate, sulfate, sulfonate, and cyanide end groups have been employed. We have also varied the moment carriers from $S = \frac{1}{2}$ (Cu) to $S = 1$ (Ni) to $S = \frac{3}{2}$ (Co) and between 1 and $\frac{3}{2}$ by synthesizing Ni–Co solid-solutions. Several of the copper salts have been described previously; some are antiferromagnet, others are metamagnets or canted antiferromagnets (20–24); the reason for the variable ground state is still unclear. The nickel compounds are all ferromagnets with Curie temperatures reaching 25 K and coercive fields less than 1000 G, and all the cobalt compounds are ferrimagnets with Curie temperature attaining 60 K and coercive fields approaching 20,000 G. Here we report the results of a representative set of this class of materials for the transition metals mentioned above with *n*-dodecylsulfonate ($C_{12}H_{25}SO_3^-$).

EXPERIMENTAL

The copper compound was prepared from $Cu_2(OH)_3(CH_3CO_2)\cdot H_2O$, which was itself synthesized by a novel procedure (25, 26) as follows. Copper acetate (10 g) was dissolved in 500 ml of distilled water and cooled in an ice bath to 10°C. A solution of NaOH (3 g) in 500 ml was made up and also cooled to 10°C. The two solutions were mixed and stirred vigorously for 10 minutes at 10°C. The mixture, in the form of a gel, was then allowed to stand at 25°C for 12 hours. Fine blue hexagonal (Fig. 1a) shaped crystals (10–20 μm in size) of $Cu_2(OH)_3(CH_3CO_2)\cdot H_2O$ were obtained with nearly 100% yield. This procedure eliminates traces of brown Cu_2O which is present when the reaction is performed at the recommended temperature of 60°C. The X-ray diffraction shows sharp lines indexable to the published monoclinic cell and there was no evidence of the unassignable peak at $d = 15$ Å (20).

$Cu_2(OH)_3(C_{12}H_{25}SO_3)\cdot H_2O$ was obtained by anion exchange: a suspension of $Cu_2(OH)_3(CH_3CO_2)\cdot H_2O$ (1 g) in a solution of $C_{12}H_{25}SO_3H$ (1 g) in 200 ml of distilled water was stirred in an air-free (to eliminate the formation of reduced species) round bottom flask for 24 hours. The shiny blue powder (Fig. 1b) was filtered, washed with distilled water and ethanol, and dried under reduced pressure.

$Ni_2(OH)_3(C_{12}H_{25}SO_3)\cdot H_2O$ and $Co_5(OH)_8(C_{12}H_{25}SO_3)_2\cdot 5H_2O$ were prepared by a direct method: the metal nitrates (3 g) and $C_{12}H_{25}SO_3H$ (2 g) were dissolved in 200 ml of a 1:1 mixture of distilled water and absolute ethanol and warmed to 40°C. To this solution was added 3 ml of ammonium hydroxide (30%) dropwise while stirring for 30–60 minutes. Light green (Ni) and darker green (Co) powders were collected, washed, and dried as described earlier. In a similar manner $Zn_5(OH)_8(C_{12}H_{25}SO_3)_2\cdot 5H_2O$, the Zn analogue of the Co compound was also prepared as a white powder.

The chemical compositions were confirmed by elemental analysis and thermogravimetric analysis.

Electron microscopy was performed on a Jeol microscope. Samples were prepared by fixing some powder onto a copper block with conducting carbon paste followed by deposition of a thin layer of conducting carbon. X-ray powder diffraction data were collected on a Seimens D-500 with Co$K\alpha$ radiation (1.789 Å). Thermogravimetric analysis was performed in air on a SETARAM TGA-DSC system. Infrared data were recorded by transmission through fine particles on a KBr plate. Temperature-dependent (4–300 K) magnetization measurements were made on a Pendulum magnetometer in fields up to 1.3 T. Isothermal field dependent magnetization data were collected on a Princeton Applied Research Vibrating Sample magnetometer (operating in field upto ± 1.6 T) and a Quantum Design SQUID (± 5 T).

RESULTS AND DISCUSSION

The copper compounds are found to be more crystalline than the nickel, cobalt, and zinc compounds. The morphologies of the copper compounds are shown in Fig. 1. The precursor compound, $Cu_2(OH)_3(CH_3CO_2)\cdot H_2O$, shows regular elongated hexagonal plates and the insertion compound, $Cu_2(OH)_3(C_{12}H_{25}SO_3)\cdot H_2O$, has the same morphology but exfoliated and rounded edges. This suggests that the rigid brucite layer is macroscopically unperturbed by the reaction which is only the replacement of the acetate groups in the galleries by the longer alkylsulfonate. The particle sizes of the nickel, cobalt, and zinc compounds are much smaller than the copper compound, and their morphologies are irrigular thin plates.

The infrared spectra are characterized by broad bands in the 3200–3500 cm^{-1} region, characteristic of the OH and H_2O vibrations. The disappearance of the vibrations due to C–O of the acetate group and appearance of the S–O bands from the sulfonate group in the spectra of the copper compounds confirm the quantitative exchange of the acetate by the sulfonate. The S–O bands show little dependence on the central metal. The slight reduction of the vibrational energies of the latter confirms its coordination of the metal atoms. The UV–vis absorption spectra of the blue copper and light green nickel compounds show very weak and broad bands at energies expected for the *d–d* transitions of the metals in an octahedral coordination of oxygen atoms. The UV–vis absorption spectrum of the green cobalt compound shows two sharp peaks at 16,600 and 17,300 cm^{-1}

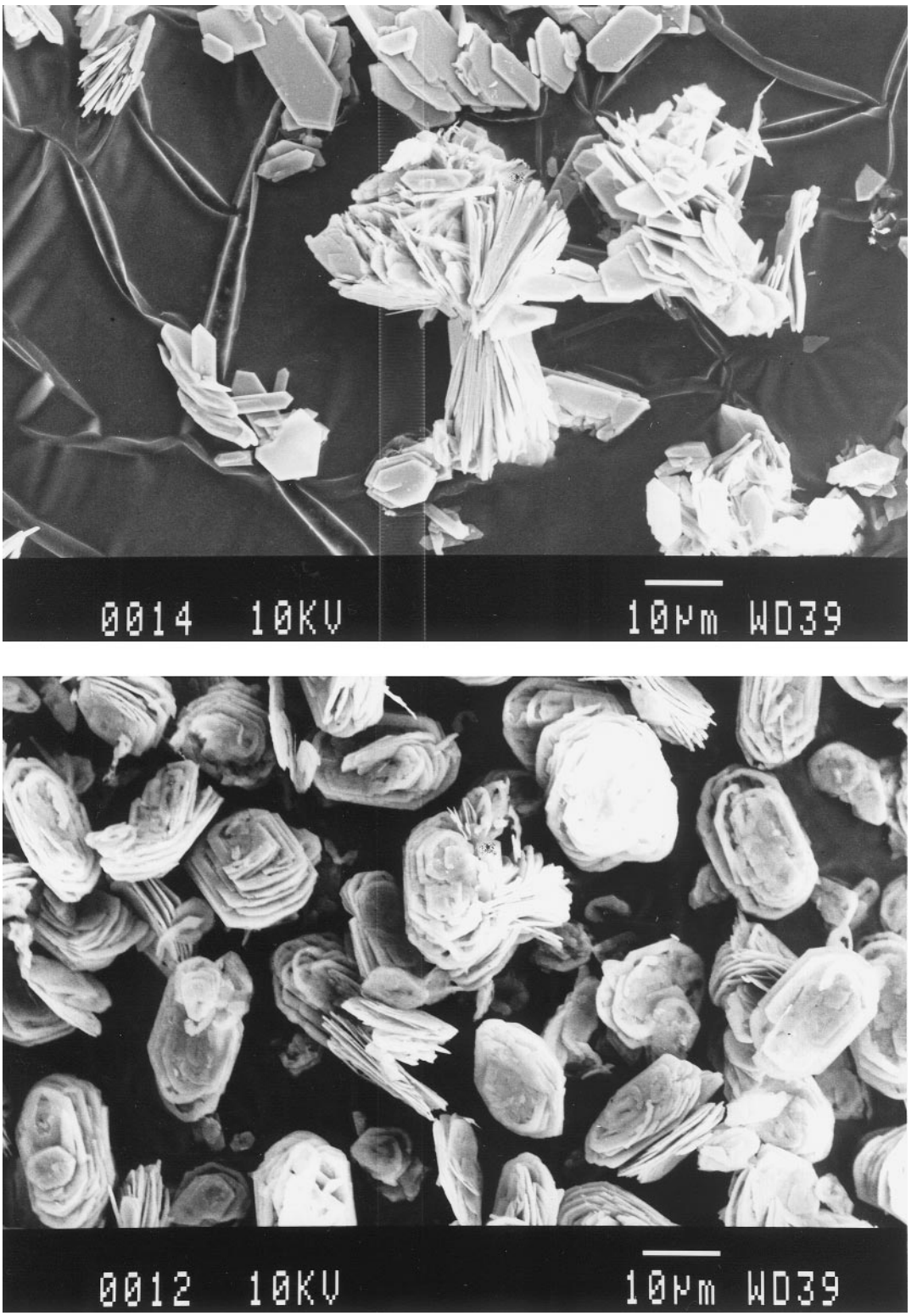

FIG. 1. Electron micrographs of (a) $Cu_2(OH)_3(CH_3CO_2)\cdot H_2O$ and (b) $Cu_2(OH)_3(C_{12}H_{25}SO_3)\cdot H_2O$.

and a broad weak band at 21,500 cm^{-1}, the latter is close to those observed for $Co_2(OH)_3NO_3$ in which all the cobalt atoms have octahedral coordination. The two intense bands are consistent with those expected for cobalt(II) in a tetrahedral coordination of oxygen (27).

The X-ray diffraction patterns of the four compounds are dominated by the 00*l* reflections, except for the copper compounds which display few additional *hkl* reflections (Fig. 2). The *a* and *b* parameters for the copper compounds are close to those reported for the monoclinic unit cell of $Cu_2(OH)_3NO_3$ (28). The *c* axis depends on the length of the alkyl chains. There is indication of loss of the solvent molecule by the appearance of a progression based on 00*l* with $l = 1$ at 20.9 Å. The nickel compound is the least crystalline and displays only up to 002 reflections. The structure of the copper and the nickel compounds may be considered to be based on brucite, $Mg(OH)_2$, where each metal site has octahedral coordination with six oxygen atoms. However, for the copper compound the Cu coordination is expected to be Jahn–Teller distorted. The alkylsulfonate anion replaces one in four of the hydroxides in the brucite and is coordinated through one of its oxygen atoms to the metal. The resulting structure is a layer of octahedral coordinated metal atoms with the alkyl chains forming a "zip or interdigitated" arrangement between layers as shown schematically in Fig. 3.

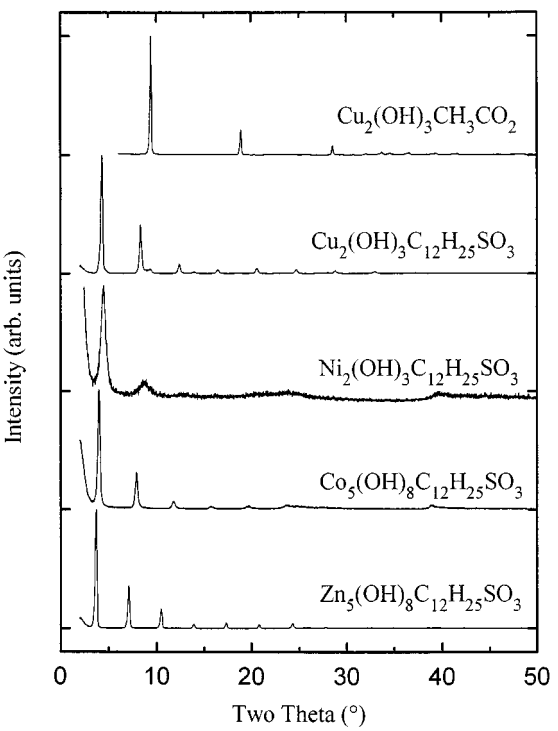

FIG. 2. Powder diffraction profiles (Co$K\alpha$, $\lambda = 1.789$ Å) showing the 00*l* progressions.

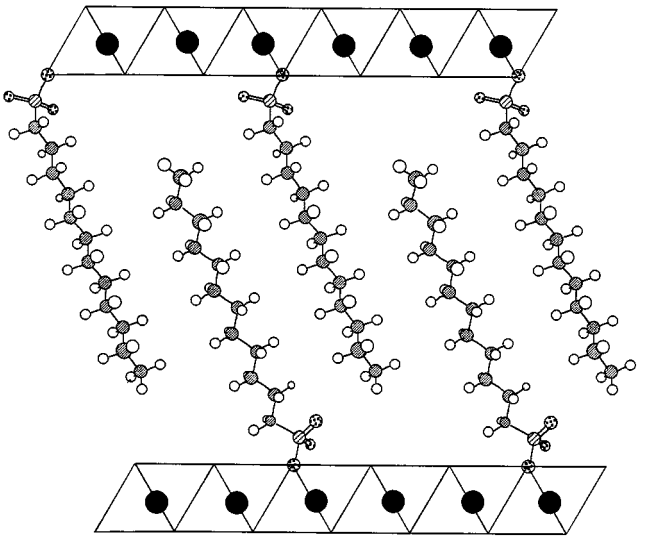

FIG. 3. Idealized single layer structure for $Cu_2(OH)_3(C_{12}H_{25}SO_3)\cdot H_2O$ and $Ni_2(OH)_3(C_{12}H_{25}SO_3)\cdot H_2O$. All the metal atoms adopt octahedral coordination.

The X-ray diffraction patterns (Fig. 2) of the cobalt and zinc compounds are identical except for a slight difference in the *d* spacing, 25.8 (Co) and 27.9 Å (Zn). There were no additional *hkl* reflections. The value of the interlayer distance and the confirmation of tetrahedral Co site in the compound by UV–vis spectroscopy would indicate that the structure of these compounds may be analogous to that found for $[Zn_5(OH)_8(H_2O)_2](NO_3)_2$ (29). The latter is also derived from brucite, where one in four of the octahedral metal atoms is replaced by two tetrahedral sites above and below the layer. The idealized structure based on the layer structure found for $[Zn_5(OH)_8(H_2O)_2](NO_3)_2$ is shown in Fig. 4. Each tetrahedral metal shares three of the bridging hydroxide ions, and its fourth coordination site is bonded by an oxygen atom of the sulfonate group. The additional thickness of the tetrahedral atoms increases the interlayer distance only marginally relative to those of the copper and nickel compounds; this may be due to a slight change in the docking angle between alkyl chain and the inorganic layer or further interpenetration of the alkyl chains.

The temperature dependence of the inverse susceptibilities and the products of susceptibility and temperature are shown in Figs. 5 and 6. The data were analyzed by fitting those in the temperature range 150–300 K ($T >$ three times the Weiss constant) to the Curie–Weiss law (30). The magnetic susceptibility measurement $Cu_2(OH)_3(CH_3CO_2)\cdot H_2O$, similar to that reported by Laget (17a), shows ferromagnetic short-range interaction above 10 K and long-range antiferromagnetic ordering at 9 K, which may be regarded as antiferromagnetic interaction between ferromagnetically coupled layers of copper(II). The insertion

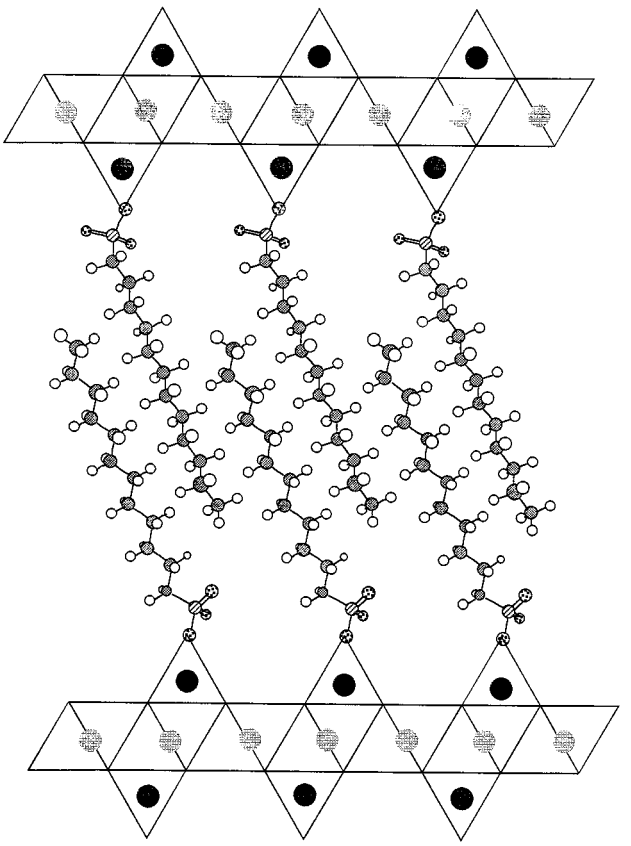

FIG. 4. Idealized triple layer structure for $Co_5(OH)_8(C_{12}H_{25}SO_3)_2 \cdot 5H_2O$, showing a single layer of octahedral cobalt sandwich by two layers of tetrahedral cobalt.

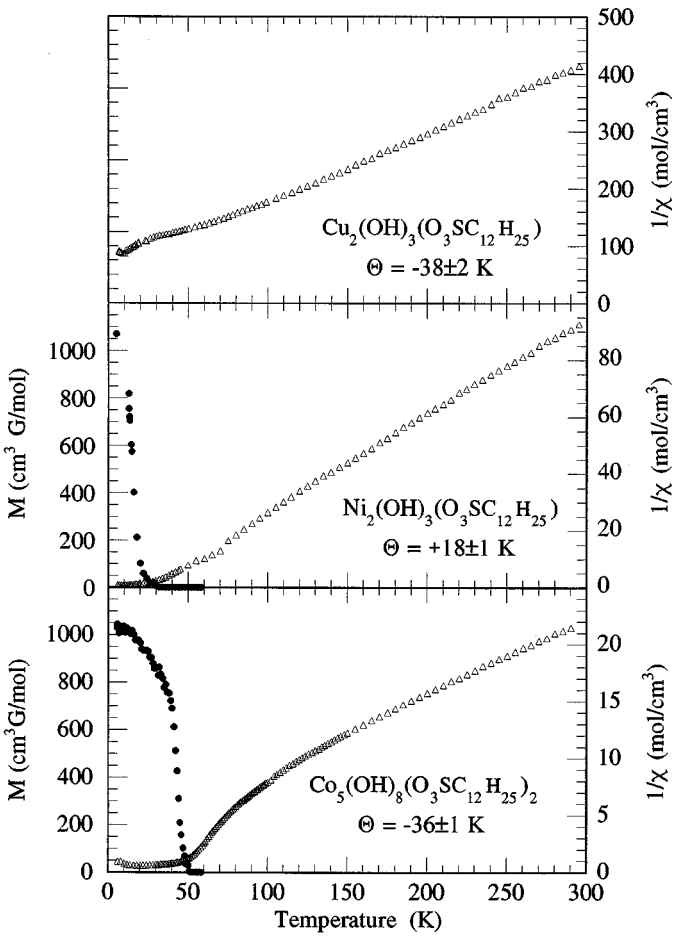

FIG. 5. Temperature dependence of the inverse susceptibilities (triangles) measured in applied field of ca. 10,000 Oe and magnetization (circles) in applied field of 200 Oe for (a) $Cu_2(OH)_3(C_{12}H_{25}SO_3) \cdot H_2O$, (b) $Ni_2(OH)_3(C_{12}H_{25}SO_3) \cdot H_2O$, and (c) $Co_5(OH)_8(C_{12}H_{25}SO_3)_2 \cdot 5H_2O$.

compound, $Cu_2(OH)_3(C_{12}H_{25}SO_3) \cdot H_2O$, shows only short-range antiferromagnetic interaction in the whole temperature range studied. The value of -38 ± 2 K for the copper compound indicates fairly strong antiferromagnetic interaction between the copper atoms within the layer. There is a slight change to a lower Weiss temperature at lower temperature. No sign of long-range order was noticed. This type of behavior was observed for the dodecyl sulfate analogue (20), while long-range magnetic ordering was observed for the dodecyl carboxylate (21). Isothermal magnetization at 4.2 K gives a linear dependence, consistent with paramagnetic behavior.

The nickel compound, on the other hand, gives a positive Weiss temperature of $+18 \pm 1$ K. Magnetization in a small field of 200 Oe shows spontaneous magnetization below 18 K. The curvature of the magnetization above the Curie temperature indicates that short range interaction extends over several nearest neighbors, thus increasing the correlation length within the layer before three dimensional ordering of the moment. The latter was confirmed by recording the isothermal magnetization in the temperature range just above the transition. Fitting the data to an effective J in the Brillouin function shows an increase of J as the temperature approach T_C. Below T_C hysteretic behavior is observed (Fig. 7), showing coercivity and remnant magnetization. The maximum value of the coercive field and remnant magnetization at 4 K are 400 Oe and 2200 cm^3 G/mol, respectively. The magnetic properties of $Ni_2(OH)_3$ $(C_{12}H_{25}SO_3) \cdot H_2O$ contrast those observed for $Ni_2(OH)_3NO_3$ which have been interpreted as metamagnetic with spin glass character (31).

The cobalt compound shows a linear dependence of the inverse susceptibility with temperature above 150 K ($\Theta = -36 \pm 1$ K). Below 150 K it decreases gradually to a minimum at 50 K. Magnetization in 200 Oe shows spontaneous magnetization below 50 K. In this case, above the transition temperature the magnetization is very small. More accurate measurements will be required in this temperature region to understand the dynamics. Isothermal magnetization measurements above the Curie temperature

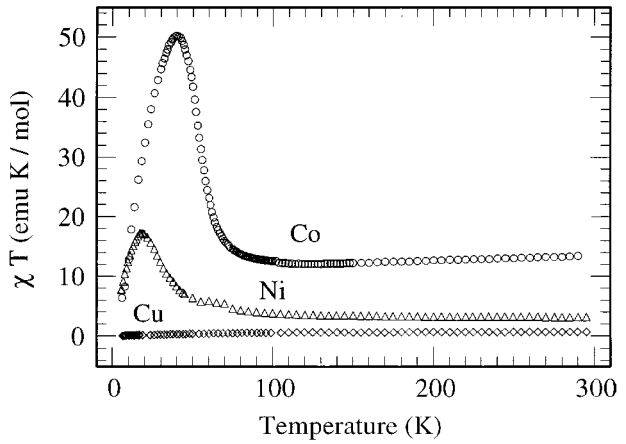

FIG. 6. Temperature dependence of the products of susceptibility and temperature measured in applied field of ca. 10000 Oe for $Cu_2(OH)_3(C_{12}H_{25}SO_3)\cdot H_2O$ (diamonds), $Ni_2(OH)_3(C_{12}H_{25}SO_3)\cdot H_2O$ (triangles), and $Co_5(OH)_8(C_{12}H_{25}SO_3)_2\cdot 5H_2O$ (circles).

are weakly field dependent. Just below the transition there is a sudden observation of hysteresis, which widens along the field axis as the temperature is lowered. At 4.2 K and in a field of 16,000 Oe the shape of the hysteresis loop is that commonly associated with primary loops, i.e., only partial reversal of the moments has been achieved (32). On going to 2 K and higher field (50,000 Oe), a symmetric hysteresis loop was observed (Fig. 7). The observed value of the coercivity field (19,000 Oe) is close to that found (18,000 Oe) for the canted antiferromagnet (33), $Fe^{II}\{N(CN)_2\}_2$, and is one of the largest for any metal–organic compound. Common to the two compounds are the large single-ion anisotropy and the shape anisotropy, the latter being plates for $Co_5(OH)_8(C_{12}H_{25}SO_3)_2\cdot 5H_2O_2$ and needles for

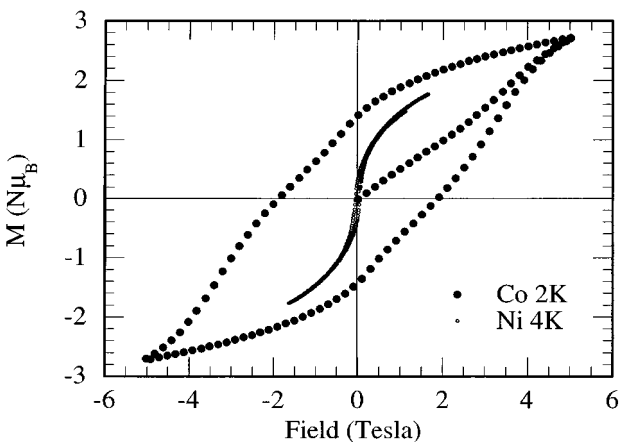

FIG. 7. Isothermal magnetization of $Ni_2(OH)_3(C_{12}H_{25}SO_3)\cdot H_2O$ at 4.2 K (open circle) and of $Co_5(OH)_8(C_{12}H_{25}SO_3)_2\cdot 5H_2O$ at 2 K (filled circle).

$Fe^{II}\{N(CN)_2\}_2$, which will have a large effect on the magnetocrystalline anisotropy. The situation is similar to the large coercivity observed in hexagonal ferrites compared to tridimensional ferrites. However, the magnetic properties are different to those reported (34) for the dodecyl sulfate analogue, $Co_2(OH)_3(C_{12}H_{25}SO_4)\cdot 2H_2O$ ($T_C = 25$ K and $H_{co} = 2000$ Oe).

The values of the Curie constants obtained from the fits are consistent with those expected for the spin only values of the three metals (30). The variable Weiss temperatures can be rationalized as follows: in the copper compound the interaction is antiferromagnetic between the copper atoms in the layer while for the nickel compound it is ferromagnetic in the layer and also between layers. The saturation magnetization for the latter is expected to be 4 $N\mu_B$ per mole. The experimental value is 1.8 $N\mu_B$ at 4 K in a field of 1.6 T, but still increasing. For the cobalt compound, the situation is more complex: there are two antiferromagnetically coupled sublattices within a layer, one comprising of cobalt in octahedral sites (3 per formula unit) and the other in tetrahedral sites (2 per formula unit). Thus the saturation magnetization per mole in the ordered state is given by

$$M_{TOTAL} = M_{OCT} - M_{TET},$$

where M_{OCT} and M_{TET} are the magnetization of the octahedral and tetrahedral sublattices, respectively, which are given by

$$M_{OCT} = 3 \times g_{OCT} \times \tfrac{3}{2} N\mu_B$$

$$M_{TET} = 2 \times g_{TET} \times \tfrac{3}{2} N\mu_B.$$

Therefore, the saturation magnetization is expected to be nearly 3 $N\mu_B$ if we assume the g values to be 2. The observed value, 2.7 $N\mu_B$ at 2 K in 50,000 Oe, is in good agreement (Fig. 7).

The most striking observation for this class of compounds is the three-dimensional long-range magnetic ordering at fairly high temperatures for spin carries in nonbonded layers separated by 25 Å. Magnetic exchange interaction through bonds will be negligible considering the number of bonds in the alkyl chains and given the crude R^{-10} dependence, where R is the distance between the spin centres. Furthermore, the long chains separating the layers are all saturated. One mechanism that has recently been proposed (35) is based on purely electrostatic dipolar interaction between the layers. The interaction energy of two magnetic dipoles is proportional to R^{-3}. It proposes that short-range interaction between the metals within the layer increases the correlation length as the temperature of the sample is lowered toward the Curie temperature. Therefore, the average effective spin per cluster (domain) becomes very large,

such that even at large distances there will be a sufficient dipole interaction to bring about long-range 3D-ordering. The critical temperature of the transition will then depend on the most dominant exchange interaction within the layer, as this defines the size of the correlated cluster. Furthermore, the critical temperature will be a very slow varying function of the distance when R is large (> 10 Å). This is a point we can verify by comparing the experimental results for compounds within the series with different interlayer distances. It appears that there is little dependence of the Curie temperatures on the interlayer spacing. For example, $Ni_2(OH)_3(N(CN)_2)$ has a d spacing of 9 Å and a T_C of 25 K (36) and for $Ni_2(OH)_3(C_{12}H_{25}SO_3)$ with $d = 23$ Å, T_C is 18 K. For the respective cobalt compounds, the d spacings are 11.5 and 24.4 Å and the T_C values are 58 and 50 K, respectively. This is in good agreement to the proposed mechanism. Furthermore, one would expect T_C to increase with the value of S of the central metal. Indeed, this is the case for all the compounds studied. We have also verified this point for mixed metal (Ni and Co) solid solutions, where a continuous increase of T_C is observed with increasing the average spin value. Furthermore, using alkyl- or aryl dicarboxylates to bridged the layers, thus introducing an exchange pathway, results in no change in properties. This, therefore, confirms that dipolar interaction at these distances is more important than exchange through bonds. The fact that we have ferromagnetically coupled layers is a good indication that the moments are perpendicular to the planes, which is expected if the spin carriers have large spin–orbit (S–O) coupling. The latter is consistent with our observation: layers in the copper compound (weak S–O) are antiferromagnetically coupled while those in the nickel (moderate S–O) and Co (large S–O) are ferromagnetically coupled. In general, the most energetically favorable configuration of a Heisenberg system when the moments are in the plane is antiferromagnetic stacking. The lack of long-range ordering for the copper compound may also be due to the lower effective S for a given cluster and to the Jahn–Teller distortion of the d^9 copper ion. Other systems that can be regarded to obey the dipolar mechanism are ammonium salts of metal chloride, A_2CrCl_4, $A =$ alkyl or aryl ammonium, which have Curie temperatures near 50 K (37, 38).

CONCLUSION

We have synthesized a series of layered magnets with variable spin value and interlayer separation. The nickel compound is a ferromagnet while the cobalt compound is a ferrimagnet as a consequence of the presence of two different coordination sites in the structure. The critical temperatures (18 and 50 K) are exceptionally high for nonbonded layers separated by 25 Å. The mechanism for magnetic ordering is proposed to be purely dipolar in character and the moments are aligned perpendicular to the planes due to the strong spin–orbit coupling. The large coercive field is most likely a consequence of synergetic alignment of crystallite shape, surface, and single-ion anisotropies.

ACKNOWLEDGMENTS

This work was funded by the CNRS-France. M.K. is grateful to the European Science Foundation for a travel grant. C.J.K. thanks Christchurch College, Oxford, for a Fellowship. We thank Prof. R. Cowley, Dr. M. J. Rosseinsky, and Dr. P. Panissod for many useful discussions.

Note added in proof. One referee wondered if the absence of the magnetic ordering in the copper salt is due to the fact that it might have a dimeric structure because the susceptibility data appear to show a broad maximum centering around 60 K. He or she also quoted the work of Bujoli *et al.* (*Inorg. Chem.* **33,** 4885 (1994)), where copper(II) phosphonates were reported, in which the structures are roughly layered but the magnetic behavior is typical of Cu(II) dimers for the hydrated salts and of one-dimensional AF Bonner–Fisher for the dehydrated ones.

Dimer or chain formation could possibly be responsible for the lack of long-range order. In the case of a dimer, the stability of a singlet ground state will depend on the angle of the bridging oxygen makes with the metals. The magnetic behavior of an AF coupled dimer will have a gap in its energy spectrum such that the susceptibility should tend to 0 at zero temperature. In the case of the copper compound presented in this paper, this is not the case; therefore the possibility is ruled out. If the compound behaves as either triangular or quadratic antiferromagnetic layers, a high-temperature series expansion or a Lines model (M. E. Lines, *J. Phys. Chem. Solids* **31,** 101, 1970), respectively, would be most appropriate. We consider the lack of a well-defined maximum in the susceptibility data would introduce large uncertainty in the refined parameters for those models. For a review on low-dimensional magnetic behavior of transition metal complexes and organic radicals, see: M. Kurmoo, P. Day, and C. J. Kepert, "Molecular Conductors and Magnets: Structure–Property Relationships. NATO ASI: Supramolecular Engineering of Synthetic Metallic Materials: Conductors and Magnets" (J. Veciana, C. Rovira, and D. Amabilino, Eds.), pp. 271–289 NATO ASI series. Vol. 518. Kluwer Academic Publishers, Boston, MA, 1998.

The referee also pointed out to another series, layered salts of $(C_nH_{2n+1}NH_3)_2Cu^{II}X_4$, where the dipolar mechanism for magnetic ordering could operate. For both this series and that of the Cr(II) series (37, 38), the Jahn–Teller effect is responsible for the near-neighbor ferromagnetic exchange.

REFERENCES

1. R. Schollhorn, "Intercalation Compounds." Academic Press, London, 1984.
2. A. Clearfield, *Chem. Rev.* **88,** 125 (1988).
3. A. J. Jacobsen, Intercalation Reactions of Layered Compounds, *in* "Solid State Chemistry: Compounds." (P. Day and A. Cheetham, Eds.). Oxford Univ. Press, Oxford, 1992.
4. D. O'Hare, Inorganic Intercalation Chemistry Chemistry, *in* "Inorganic Materials" (D. W. Bruce and D. O'Hare, Eds.). Wiley, London, 1993.
5. A. Clearfield, *Curr. Opin. Solid State Chem.* **1,** 268 (1996).
6. T. Pinnavaia, *Science* **220,** 365 (1983).
7. T. Shichi, K. Takagi, and Y. Sawaki, *J. Chem. Soc., Chem. Commun.* 2027 (1996).
8. I. V. Mitchell, "Pillared Layered Structures; Current Trends and Applications." Elsevier, London, 1990.
9. C. P. Poon, *J. Haz. Mater.* **55,** 159 (1997).

10. A. Clearfield, "Inorganic Ion Exchange Materials" (A. Clearfield, Ed.). CRC Press Inc., Boca Raton, FL, 1991.
11. M. Jakupca and P. K. Dutta, *Chem. Mater.* **7,** 989 (1995).
12. S. Carlino, *Solid State Ionics* **98,** 73 (1997).
13. S. Carlino, *Chem. Br.* **33,** 59 (1997).
14. S. P. Newman and W. Jones, *New J. Chem.* **22,** 105 (1998).
15. K. Binder and A. P. Young, *Rev. Mod. Phys.* **58,** 801 (1986).
16. L. J. De Jongh (Ed.), "Magnetic Properties of Layered Transition Metal Componds." Kluwer Academic Publishers, Dordrecht, 1990.
17. (a) V. Laget, Thèse doctorat, Universite Louis Pasteur, Strasbourg, France (unpublished), 1998. (b) M. Drillon, C. Hornick, V. Laget, P. Rabu, F. M. Romero, S. Rouba, G. Ulrich, and R. Ziessel, *Mol. Cryst. Liq. Cryst.* **273,** 125 (1995).
18. Y. Honda, Y. Hirayama, and M. Futamoto, *IEEE Trans. Magnetics* **34,** 1633 (1998).
19. W. Feitknecht, A. Kummer, and J. W. Feitknecht, "16th Int. Congr. Pure Appl. Chem.," p. 243. Mem. Sect. Chim. Minerale, Paris, 1958.
20. (a) S. Rouba, Thèse doctorat, Universite Louis Pasteur, Strasbourg, France (unpublished), 1996. (b) P. Rabu, S. Rouba, V. Laget, C. Hornick and M. Drillon, *J. Chem. Soc., Chem. Commun.* 1107 (1996).
21. W. Fujita and K. Awaga, *Inorg. Chem.* **35,** 1915 (1996).
22. V. Laget, P. Rabu, C. Hornick, F. Romero, R. Ziessel, P. Turek, and M. Drillon, *Mol. Cryst. Liq. Cryst.* **305,** 291 (1997).
23. V. Laget, M. Drillon, C. Hornick, P. Rabu, F. Romero, P. Turek, and R. Ziessel, *J. Alloys Compounds* **262,** 423 (1997).
24. M. A. Girtu, C. M. Wynn, W. Fujita, K. Awaga, and A. J. Epstein, *Phys. Rev. B* **57,** R11058 (1998).
25. R. M. A. Lieth, "Preparation and Crystal Growth of Materials with Layered Structure," Dordrecht, Boston, MA, 1977.
26. M. Meyn, K. Beneke, and G. Lagaly, *Inorg, Chem.* **32,** 1209 (1993).
27. A. P. B. Lever, "Inorganic Electronic Spectroscopy," Elsevier, Amsterdam, 1986.
28. H. Effenberger, *Z. Kristallogr.* **165,** 127 (1983).
29. (a) W. Stahlin, *Acta Crystallogr., Sect. B* **26,** 860 (1970). (b) P. Benard, J. P. Auffredic, and D. Louer, *Thermochem. Acta* **232,** 65 (1994).
30. O. Kahn, "Molecular Magnetism." VCH Publishers Inc., New York, 1993.
31. S. Rouba, P. Rabu, E. Ressourche, L. P. Regnault, and M. Drillon, *J. Mag. Mater.* **163,** 365 (1996).
32. S. Chikazumi, "Physics of Magnetism." Wiley, New York, 1978.
33. M. Kurmoo and C. J. Kepert, *New J. Chem.* December (1998).
34. V. Laget, S. Rouba, P. Rabu, C. Hornick, and M. Drillon, *J. Magn. Magn. Mat.* **154,** L7 (1996).
35. M. Drillon and P. Panissod, *J. Magn. Magn. Mat.* **188,** 93 (1998).
36. M. Kurmoo, unpublished results.
37. M. J. Stead and P. Day, *J. Chem. Soc., Dalton Trans.* 1081 (1982).
38. C. Bellitto and P. Day, *J. Chem. Soc., J. Mater. Chem.* **2,** 265 (1992).